Green Chemistry

Fast and solvent free polymerization of carbohydrates induced by non-thermal atmospheric plasma

SCHOLARONE™
Manuscripts

Green Chemistry

ARTICLE

Fast and solvent free polymerization of carbohydrates induced by non-thermal atmospheric plasma

Joakim Delaux,[a,b] Michaël Nigen,[b] Elodie Fourré,[a] Jean-Michel Tatibouët,[a] Abdellatif Barakat,[b] Loyda Atencio,[c] José M. García Fernández,[c] Karine De Oliveira Vigier[a] and François Jérôme*[a]

Non-thermal atmospheric plasma (NTAP) is a physical technology that has been previously employed for surface treatment (cleaning, coating, erosion, etc.) and water or air depollution. We show here that, beyond surface effects, NTAP is capable of enabling the complete and fast polymerization of various mono- and disaccharides in the solid state within only few minutes and at low temperature (40-80°C). NTAP-induced polymerization involves a radical mechanism and yields water soluble polysaccharides with a mean molar mass up to 100 000 g/mol and a mean hydrodynamic radius of 3 nm. Although polymerization reactions promoted by NTAP occurs in a randomly manner, the α-1,6 and β-1,6 linkages are however dominant. Furthermore, we discovered that NTAP is highly selective, strongly favoring glycosylation over other chemical transformations in the bulk. Under our working conditions, glycosyl units are preserved and constitute the repeating units of the polysaccharide product. No chemical degradation (e.g. intramolecular dehydration reactions) was observed, allowing a white powder to be recovered with a yield higher than 93 wt%. From a practical point of view, NTAP has a great potential of breakthrough in the production of polysaccharides, notably because it does not require the use of solvent or catalyst, thus by-passing the traditional post-treatment of aqueous effluents and catalyst recycling characteristic of biotechnological polysaccharide production. Its efficiency at low temperature also prevents carbohydrates from degradation. Last, NATP proceeds on an on/off switch basis, allowing the polymerization reaction to be started and stopped quasi instantaneously.

Introduction

Polysaccharides are chemicals of paramount importance in our society and have a high potential of market in various industrial sectors such as materials, pharmaceutic, cosmetic or food industries. Theoretically, carbohydrates can be polymerized in the presence of an acid catalyst (so-called reversion reaction).[1] However, these pathways suffer from poor energy efficiency and a lack of selectivity. Indeed, acid catalysts also enhance side reactions that have similar apparent activation energy than the polymerization reaction (e.g., successive intramolecular dehydration). Biocatalytic routes are more selective and generally preferred for the synthesis of polysaccharides.[2] However, enzymatic processes suffer from a lack of productivity and high dilution ratios inducing costly downstream purification processes.

Here, we report a cross-disciplinary work at the border of chemistry and physics based on the utilization of non-thermal atmospheric plasma (NTAP). We discovered that this technology was capable of selectively polymerizing carbohydrates quasi instantaneously upon command without assistance of any solvent or catalyst or external source of heating. This technology not only improves profitability through increase of reaction yield, decrease of reaction times and the reduction of solvent waste but also opens a convenient access to valuable polysaccharides that are hardly accessible by conventional routes.

NTAP is an ionized gas that can be obtained by applying a high difference of potential between two electrodes isolated each other by a dielectric.[3] Under a gaseous atmosphere, electrons are accelerated by the electric field and collide with neutral molecules in the gas phase, which generate highly active species (atoms, ions, electrons, free radicals, photons, etc.). NTAP is a non-equilibrium plasma i.e. the temperature of electrons is much higher than that of the gas. Consequently, NTAP takes place at near ambient temperature, which is of huge interest notably for carbohydrate conversion. The NTAP technology has been used since a long time for surface treatment (cleaning, coating, erosion, etc.) and water or air depollution.[4] In the field of surface coating, polymerization assisted by plasma is often employed.[4d] In this case, volatile and ionisable monomers are required to go to the plasma

a. Institut de Chimie des Milieux et Matériaux de Poitiers, CNRS/Université de Poitiers, ENSIP, 1 rue Marcel Doré, Bat 1, TSA 41105, 86073 Poitiers Cedex 9, France. E-mail: francois.jerome@univ-poitiers.fr.
b. INRA, UMR 1208 Ingénierie des Agropolymères et Technologies Emergentes (IATE), 2 Pierre Viala, Montpellier F-34060 France.
c. Instituto de Investigaciones Químicas (IIQ), CSIC - University of Sevilla, Avda. Americo Vespucio 49, E-41092 Sevilla, Spain.
Electronic Supplementary Information (ESI) available: experimental procedures, copy of RAMAN, NMR, XRD, XPS, MALDI-TOF spectra, SEC/MALS data and weight loss. See DOI: 10.1039/x0xx00000x

state. As a consequence, only low molecular weight apolar building blocks such as furan, acrylonitrile, styrene or acetylene, to mention few, are eligible. In addition, polymers produced by plasma are actually graft polymers since they have to grow on a solid support. Regarding natural materials such polysaccharides (cellulose fibers, starch, chitosan),[5] NTAP has been essentially used to modify their surface hydrophilicity, mechanical strength, surface erosion, surface roughness, etc. The mechanism at play during the treatment of polysaccharides by NTAP implies the formation of radical species, as previously demonstrated by Electron Spin Resonance (ESR).[5b,6] which leads to oxidation, dehydroxylation reactions, ring opening, etc. [7-10, 6b,] Due to the tight hydrogen bond network of polysaccharides, these radical species does not diffuse within the bulk and thus NTAP only impacts the surface of these natural materials.

To the best of our knowledge, the use of NTAP for the production of valuable fine chemicals such as polysaccharides remains unexplored. Indeed, NTAP is nowadays mostly employed for surface modification in the field of material science or depollution. This manuscript explores, for the first time, the versatility of NTAP as a physical technology for the solvent and catalyst free polymerization of various saccharides. Thanks to a weaker hydrogen bond network than that of polysaccharides, radicals generated on the surface of saccharides by NTAP induce a deep and fast polymerization by propagation reaction in the bulk yielding, in few minutes, valuable polysaccharides. Furthermore, this physical technology is highly selective towards glycosylation reaction and no downstream purification process is further required, polysaccharides being directly recovered as a white powder at the end of the NTAP treatment.

Results and discussion

Polymerization of mannose induced by NTAP

To demonstrate the potential of this technology for the synthesis of polysaccharides, mannose was first selected as a representative carbohydrate. The applications of mannans and mannan oligosaccharides in the food industry are well known, and their description is out of the scope of this study.[11] Typically, a powder of mannose was placed between two parallel square-electrodes (copper) of 25 cm^2 isolated from each other by a dielectric material (commonly named dielectric barrier discharge (DBD) reactor).[8] To maintain an optimal plasma discharge, the gap between both electrodes was fixed to 4 mm. To create the plasma discharge, a bipolar pulse signal was used at a maximum voltage of 9.5 kV at 2.2 kHz frequency (*i.e.* 15 W). All reactions were conducted under air at a flow rate of 100 mL/min. During the NTAP treatment, samples of mannose were taken from the DBD reactor after 10, 15 and 30 min of NTAP treatment and analyzed by size exclusion chromatography (SEC). Fig. 1 shows that mannose was nearly completely consumed after 15 min of NTAP treatment and products with a higher molecular weight were produced.
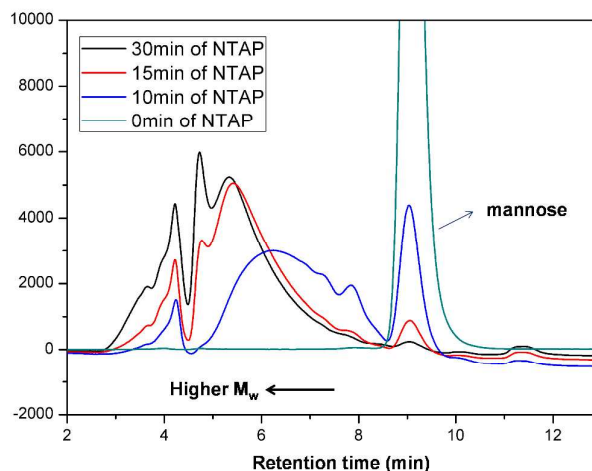

Fig. 1. Conversion of mannose monitored by Size Exclusion Chromatography. All samples were analyzed at a similar concentration

Monitoring of the reaction by Mass Assisted Laser Desorption Ionization/Time of flight (MALDI-TOF) supported the polymerization of mannose in the DBD reactor (Fig. S1). Signals are repeated every 162 uma, suggesting that the chemical structure of the mannopyranosyl units is preserved in the polymer structure. The polymerization of mannose can be also indirectly observed by X-ray diffraction (XRD) and ^{1}H/^{13}C NMR (Fig. S2). Indeed, an important enlargement of signals was observed in both cases which are often the signature of a random polymerization. More information on the characterization of the recovered polymannoside is provided later in the manuscript.

Interestingly, one can notice from MALDI-TOF analyses (Fig. S1) that the polymerization reaction was enhanced after 7 min of NTAP treatment time. To get a deeper insight on this phenomenon, we monitored the conversion of mannose as a function of the NTAP treatment time (Fig. 2a, black line). In agreement with MALDI/TOF observations, an induction period of 7 min was observed after which mannose was completely polymerized within 3 min. This period of induction was found to be linked to the increase of the DBD reactor temperature (assured by the dissipated energy). Notably, this period of induction fitted well with the time required by the DBD reactor to reach 40°C (Fig. 2a, dashed line).[12] To support this observation, the DBD reactor was placed in a freezer and the starting temperature was decreased down to -23°C prior to starting the NTAP treatment. Under these conditions, the time required by the DBD reactor to reach 40°C was increased from 7 to 15 min which is also concomitantly accompanied by an increase of the induction period time from 7 to 15 min (Fig. 2b). Similarly, when the DBD reactor was initially heated at 65°C or 75°C prior to starting the NTAP, no induction period was observed. Finally, when the NTAP treatment was successively stopped and started again to maintain the DBD reactor at a temperature lower than 40°C, no polymerization took place and mannose remained unaltered. Altogether, these results suggest that the polymerization of mannose induced by NTAP starts when the DBD reactor reaches 40°C.

One can see in Fig.2b that the polymerization rate remained similar (32 mg/min) whatever the starting temperature of the DBD reactor (40°C or 65°C or 75°C), suggesting that the apparent activation energy of the reaction was very low. This kinetic behavior discards a classical acid-promoted reversion pathway and is instead fully consistent with a radical mechanism.
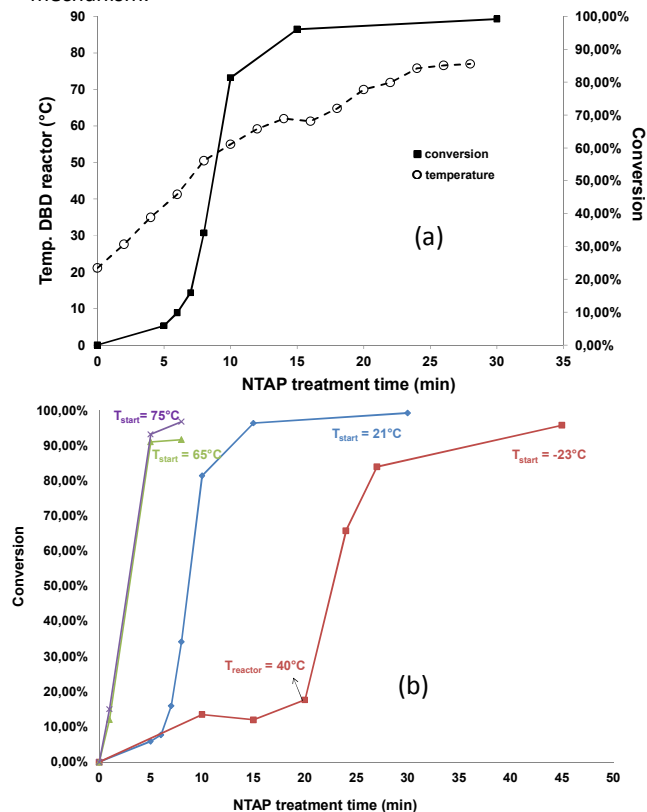

Fig. 2. (a) conversion of mannose (black line) *vs* NTAP treatment time and the temperature of the DBD reactor (dashed line) and (b) influence of the starting temperature of the DBD reactor on the induction period.

The frequency applied during the NTAP treatment has a direct impact on the temperature ramp rate of the DBD reactor and consequently on the conversion rate of mannose. For instance, at 1 kHz, the temperature of the DBD reactor did not exceed 40°C even after 10 min of NTAP treatment and, as expected, no conversion of mannose was observed. Conversely, at 3 kHz, the temperature of the DBD reactor reached 62°C and 92°C after 5 min and 10 min of NTAP treatment, respectively. As a consequence, at 3 kHz, 75% of mannose was converted after 5 min of NTAP treatment *versus* only 5% at 2.2 kHz.

Then, we checked the carbon mass balance of the reaction by weighting the amount of polymannosides recovered after 15 min of NTAP treatment. The weight loss caused by the release of water during the polymerization of mannose should be theoretically around 15 wt%. A weight loss of 22 wt% was observed which is in the expected range (Fig. S3). The difference mostly stems from the loss of material when recovering the powder of polymannosides from the DBD reactor. Note that the weight loss increased rapidly to 15 wt% between 7 and 10 min of NTAP treatment and then did not

change, which indicates that (1) the polymerization of mannose during this period is accompanied by a release of water and (2) the polymannosides thus formed remain stable under NTAP treatment. In other words, it means that, at least, 93 wt% of the mannopyranosyl units were preserved during the NTAP treatment.

To further support the above claim, the DBD reactor was coupled to a mass spectrometer (MS) to analyze on-line the gas flow at the exit of the DBD reactor. Production of water was clearly evidenced by MS which is fully consistent with the polymerization of mannose. CO_2 was also detected but its amount was found very low (less than 1 % yield relative to the amount of mannose) supporting the stability of the mannopyranosyl unit during the NTAP treatment. One should also note that no formaldehyde or formic acid was detected in the gas phase.

Structure of polymannosides

Polymannosides were analyzed by means of different technics. First, FT/IR and RAMAN spectroscopies were employed. No signals characteristic of a C=O or C=C bond was observed and both spectra remained similar to that of mannose, reinforcing the hypothesis drawn above regarding the oligomannosyl character of the product (Fig. S4). Solid ^{13}C CP MAS and liquid NMR (in D_2O) further supported this claim and no peaks ascribable to C=O group was observed (more information on ^{13}C CP/MAS NMR is provided later). To get a closer view on this aspect, polymannosides were then analyzed by X-ray photoelectron spectrometry (XPS), which provides information on the chemical composition of the surface of a material (in a layer of 10 nm). In agreement with previous results on the treatment of polysaccharides by NTAP,[5-7] XPS revealed a certain degree of oxidation of the polymannoside particle surfaces, with the presence of -O-C=O groups in a relative ratio of about one -O-C=O groups each three mannosyl units ((Fig. S5). Although not clear at the moment, the absence of oxidation in the bulk is however consistent with previous results and might be ascribed (1) to the formation of radicals of different nature in the bulk and on the surface which is in direct contact with the NTAP gas and/or (2) caging effects of the surface.[5-7]

To get more insight on the chemical structure of the polymannosides formed after NTAP treatment of mannose, the disaccharide fraction was investigated in depth by means of gas chromatography (GC). The analyses were conducted on a sample having a conversion of mannose of 43%, in order to get quantifiable signals, following derivatization of the sugars into the corresponding aldononitrile peracetates.[13] Using commercial standards, the presence of all possible reducing mannobioses, namely the α- and β-(1,2), (1,3), (1,4) and (1,6)-linked mannodisaccharides, was established and their relative proportions were determined. The relative distribution of all positional isomers is provided in Fig. 3. (see also Supporting information for experimental details).[14] All hydroxyl groups of mannose are thus engaged in the first steps of the NTAP-
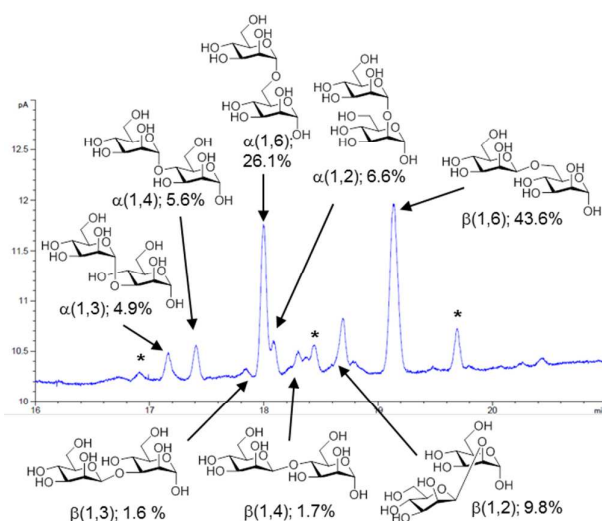
Fig. 3. GC chromatogram of polymannoside (mannodisaccharide region; 10% of the total polymannoside sample) after derivatization into the corresponding aldononitrile peracetates (see Supporting information). The structural assignment (comparison with authentic standards) is shown. The relative proportions of the different isomers, calculated from the corresponding response factors relative to the internal standard (phenyl β-D-glucopyranoside; see Supporting information) are also indicated.

promoted oligomerization reaction. The formation of glycosidic linkages involving the primary hydroxyl group (OH-6) was however dominant (71%), with a notable preference for β-1,6 (44%) *versus* α-1,6 (27%) bond formation.

Higher mannose oligomers are also formed by subsequent glycosylation reactions, which may occur at either the terminal non reducing mannopyranosyl unit, at an inner fragment in the chain or at the reducing end. In the first and third cases a linear structure (reducing or not reducing, respectively) is obtained, whether in the second case a branching point is introduced in the skeleton. To assess the degree of branching, the mixture of polymannosides was subjected to a methylation (MeI/NaOH)[15]-hydrolysis (TFA, 120°C)-deuteroboration (NaBD$_4$)-acetylation (Ac$_2$O/TFA) sequence[16] prior to GC-MS analysis. This protocol affords the corresponding alditols labelled with deuterium at C-1, methylated at non-glycosylated positions and bearing acetyl groups at positions that were glycosylated in the starting polymer, which can be unequivocally assigned from the corresponding fragmentation patterns in MS by comparison with authentic standards.[17] The
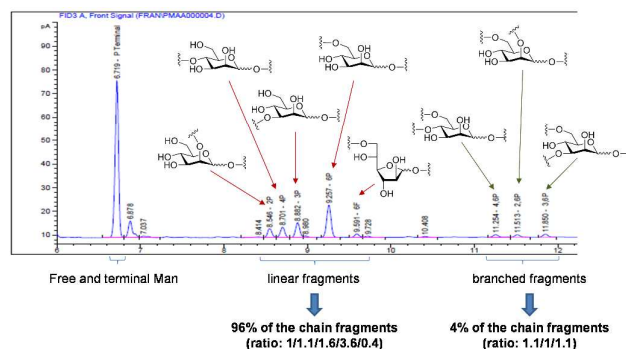

Fig. 4. Analysis of the branching degree by means of GC/MS analyses using the methylation-hydrolysis-deuteroboration-acetylation sequence

data indicated that monoglycosylated residues accounted for as much as 96% of the inner chain mannosyl units, with only 4% of inner mannosyl fragments doubly glycosylated (2,6-, 3,6- and 4,6-di-O-mannosylated residues), supporting that the structure of the oligosaccharides is essentially linear (Fig. 4). The chain grows preferentially through the primary position (O-6). Nevertheless, glycosylation at secondary positions (O-2, O-3 and O-4) represents altogether 50% of the total (Fig. 4).

From the above study, it is clear that quite randomly polymerized macromolecules were produced by NTAP treatment, rationalizing the enlargement of signal observed by XRD and ^{1}H/^{13}C NMR. It is worth mentioning that the GC analysis did not reveal oxidized fragments (up to 15 min of NTAP treatment) further reinforcing the notion that oxidation of mannose occurred on a thin layer at the surface of particles and not in the bulk.

More information on the structure of the polymannosides was obtained from the corresponding ^{13}C CP/MAS NMR spectrum.[18,19]. The chemical shift of the carbon atoms together with the absence of C=O group confirms the oligomannosyl character of the product (Fig. S6). The crystallinity index of the polymannosides was estimated by deconvolution of the ^{13}C CP/MAS NMR spectrum.[20] Notably, crystalline and amorphous peaks of C4 were clearly evidenced at 84.6 and 77.4 ppm, respectively. Integration of these peaks revealed that the crystallinity index of polymannoside was very low (<5%) which is fully consistent with XRD analysis described above.

Produced polymannosides were then analyzed by size exclusion chromatography coupled to multi-angle light scattering (SEC-MALS) to get more information at the macromolecular level (Fig.5).
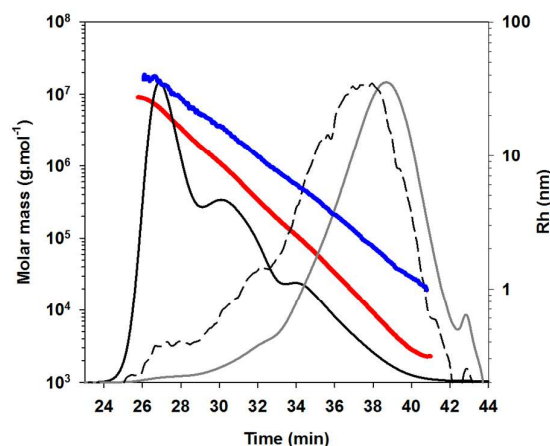

Fig. 5. SEC MALS chromatograms (LS 90°: black line; RI: grey line; specific viscosity: dotted line) with molar mass (g.mol-1, red line) and Rh (nm, blue line) distributions for polymannoside sample. Macromolecules were eluted using 0.1 M LiNO3 containing 0.02% NaN3.

The elution profiles (Light Scattering (LS) at 90° and Refractive index (RI) signals) displayed at least three main populations differing by their proportion and hydrodynamic volume, reflecting a polydisperse sample. SEC MALS experiments revealed the formation of a continuum of polymerized mannose macromolecules with molar mass ranging from 2×10^3 to 9×10^6 g·mol^{-1} and hydrodynamic radii ranging from

1.2 to 37.2 nm. Recovered polymannoside was characterized by a mean molar mass (Mw) of 95590 g.mol^{-1}, a mean intrinsic viscosity (η) of 7.7 ml.g^{-1} and a calculated hydrodynamic radius (Rh) of 3.3 nm (Table 1). Polymannoside displayed a high polydispersity index (M_w/M_n) value of 15 which is fully consistent with a random polymerization of mannose (Table 1).

The conformation of polymannosides was further investigated by plotting the Rh value *vs* the M_w.[21] The Rh and M_w values are linked together and obey to the equation (1) where Rh and M_w are the hydrodynamic radius and the molar mass, respectively, v_h is the hydrodynamic coefficient and K_h is a constant.
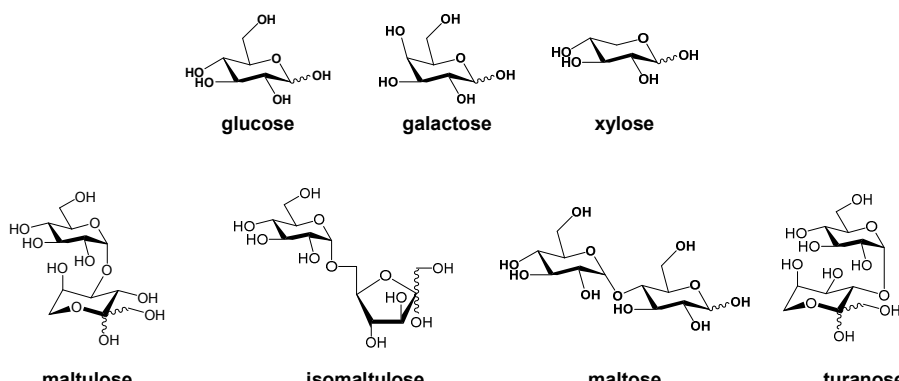
$$Rh = K_h M_w^{v_h}$$ Equation (1)

The hydrodynamic coefficient depends on the overall shape of the macromolecule (especially anisotropy), temperature and macromolecule-solvent interaction. Theoretical v_h values are 0.33 for a sphere, 0.5-0.6 for a linear random coil and 1 for a rod.[21] The plot of Rh *vs* M_w displayed a linear relationship giving a hydrodynamic coefficient of 0.43 (Fig. S7). This linear relationship means that the different polymannosides in the heterogeneous sample exhibit a similar conformation whatever their degree of polymerization. Importantly, a v_h value of 0.43 suggests that polymannoside adopted a conformation between a hard sphere and a random coil. This value is in accordance with a compact conformation similar to that observed in star polymers or dendrimers,[22] in spite of a

relatively low branching degree as determined by GC-MS analysis of the corresponding methylation-hydrolysis-reduction-acetylation product. The random polymerization of mannose together with a branching degree of 4% may rationalize the compact architecture. Furthermore, one should note that a small proportion of branching points can give rise to a star-like architecture if they are located at the beginning of the chain, which is probably favor due to lower steric constrains at the early stages of the oligomerization process. This conclusion is further reinforced by the very high solubility of the polymannoside in water (850 g/L).

Scope of the NTAP for carbohydrate polymerization

In order to explore the scope and limitations of the NTAP technology to promote reversion reaction of carbohydrate substrates and afford glycopolymer materials, three more monosaccharides and four disaccharides were tested under the experimental conditions used for mannose polymerization. Because the induction period depends on the reactivity of each saccharide, the NTAP treatment was arbitrarily stopped after 30 min in all cases. Results are summarized in Table 1. To our delight, the NTAP was capable of oligomerizing all tested carbohydrates. When disaccharides were employed, it was found by MALDI-TOF analyses that disaccharidyl moieties constituted the repeating unit of the oligomers suggesting that disaccharides were not cleaved during the NTAP treatment.

Table 1. Polymerization of various saccharides induced by NTAP

Saccharides	Time of induction (min)	Temp. of polymerization (°C)	Conv. (%)	M_w (g/mol)	M_n (g/mol)	Đ	DP	Rh (nm)	η (ml/g)	v_h
Glucose	15	66	70	5051	909	5.6	33	1.4	5.0	0.41
Xylose	10	56	90	5368	1121	5.3	45	1.4	5.3	0.42
Galactose	20	72	62	3378	302	11.2	28	0.8	3.5	0.44
Maltulose	7	40	92	3723	1746	2.1	26	1.2	4.2	0.4
Maltose	10	56	91	2325	835	2.8	15	1.0	4.2	0.42
Isomaltulose	15	66	87	3409	1207	2.8	25	1.0	3.5	0.38
Turanose	30	80	80	2214	581	3.8	18	0.8	3.2	0.37

Green Chemistry

ARTICLE

The mean M_w was in the same range for all samples, with values ranging from 2000 to 5500 g·mol^{-1} along with a polydispersity ranging from 2 to 11 (Table 1). M_w values are significantly lower than those collected from mannose, for which NTAP-promoted reversion was optimized in this work. Of course, these conditions might well not represent the optimized conditions (temperature, frequency, time, etc.) for all tested carbohydrates in Table 1, since the structure of saccharides directly affect the nature of radical species[23] and thus the polymerization reaction. Nevertheless, results collected in Table 1 clearly highlight the potential of NTAP for the polymerization of carbohydrates under dry conditions.

The conformation of the glycopolymers obtained from the mono and disaccharides presented in table 1 was further investigated by building the corresponding Rh *vs* M_w plots. As for the polymannoside case, a linear relationship was observed for all of them. Notably, the mean ν_h value was around 0.40, with individual values ranging from 0.37 to 0.44 (Table 1), indicating that (1) the produced polysaccharides have similar macromolecular structures and (2) they adopt a compact organization compatible with a random polymerization of the sugar (Fig. S8).

Conclusion

NTAP can be regarded as a physical stimulus to induce, within few minutes only, the fast and complete poly(oligo)merization of various mono- or disaccharides without assistance of any solvent or catalyst. Reversion reactions leading to glycosidic linkage formation between sugar moieties are strongly favored over oxidation or dehydration processes under these conditions. Although the polymerization occurs in a randomly manner, the α-1,6 and β-1,6 linkages have been found to be dominant. Under our working conditions, polysaccharides were recovered as a white powder with a yield higher than 93 wt%

The NTAP process is distinguished from conventional routes in that it is efficient at low temperatures, it does not need an external source of heating or catalyst or solvent and it leads to fast and effective conversions under air. Furthermore, NTAP activation of carbohydrates functions on an on/off switch basis, allowing the polymerization reaction to be started and stopped quasi instantaneously. As compared to conventional (bio)catalytic routes the favorable characteristics of NTAP-promoted carbohydrate oligomerization allows by-passing (1) the post-treatment for aqueous effluents and catalyst recycling, and (2) high dilution ratios, two main bottlenecks of the former technologies. More generally, NTAP provides an

efficient mean to produce valuable water-soluble polysaccharides from a diverse array of mono- and disaccharides.

Further work is still needed to fully disclose the mechanisms at play during NTAP-promoted glycopolymerization. Nevertheless, we do believe that the body of results here presented convincingly illustrates the great potential of breakthrough of the technology not only for the production of polysaccharides with original structures but also for the polymerization of solid monomers in general. Research in that direction is currently pursued in our laboratories.

Notes and references

1   (a) H. M. Pilath, M. R. Nimlos, A. Mittal, M. E. Himmel, D. K. Johnson, *J. Agric. Food Chem*., 2010, **58** (10), 6131–6140. (b) R. F. Helm, R. A. Young, A. H. Conner, *Carbohydr. Res*., 1989, **185**(2), 249-260. (c) H. M. Pilath, W. E. Michener, R. Katahira, A. Mittal, J. M. Clark, M. E. Himmel, M. R. Nimlos, D. K. Johnson, *Energy & Fuels,* 2013, **27**(12), 7389-7397

2   (a) J. A. Akkara, M. S. R. Ayyagari, F. F. Bruno, *Trends Biotechnology*, 1999, **17**(2), 67-73. (b) L. Ferreira, M. H. Gil, J. S. Dordick, *Biomaterials,* 2002, **23**(19), 3957-3967. (c) J.-I. Kadokawa, *Chem. Rev*., 2011, **111** (7), pp 4308–4345

3   As selected reviews, see: (a) E. Moreau, *J. Phys. D Appl. Physics,* 2007, **40**(3), 605-636. (b) M. Moreau, N. Orange, M. G. J. Feuilloley, *Biotechnol. Adv*., 2008, **26**(6), 610-617. (c) A. M. Vandenbroucke, R. Morent, N. De Geyter, C. Leys, *J. Hazard. Mater*., 2011, **195**, 30-54. (d) V. Rat, A. B. Murphy, J. Aubreton, M. F. Elchinger, P. Fauchais, *J. Phys. D Appl. Physics,* 2008, **41**(18), 183001-183029. (e) A. M. Bykov, M. A. Malkov, J. C. Raymond, A. M. Krassilchtchikov, A. E. Vladimirov, *Space Sci. Rev*., 2013, **178**(2-4), 599-632.

4   (a) L. Bardos, H. Barankova, *Thin Film Solid,* 2010, **518**(23), 6705-6713; (b) A. M. Vandenbroucke, R. Morent, N. de Geyter, C. Leys, *J. Hazard. Mater*., 2011, **195**, 30-54; (c) C.

Tendero, C. Tixier, P. Tristant, J. Desmaison, P. Leprince, *Spectrochim. Acta B.*, 2006, **61**(1), 2-30; (d) P. Cools, S. Van Vrekhem, N. De Geyters, R. Morent, *Thin Solid Films,* 2014, **572**, 251-259.

5 As selected articles, see: (a) L.C. Vander Wielen, Max Östenson, Paul Gatenholm, Arthur J. Ragauskas, *Carbohydr. Polym.*, 2006, **65** (2), 179-184. (b) K. Johansson in Plasma Technologies for Textiles, (Ed. R. Shishoo), 2007, Woodhead Publishing Limited, Cambridge. (c) E. Bozaki, K. Sever, M. Sarikanat, Y. Seki, A. Demir, E. Ozdogan, *Compos. Part B,* 2013, **45**, 565-572. (d) E. Nithya, R. Radhai, R. Rajendran, S. Shalini, V. Rajendran, S. Jayakumar, *Carbohyr. Polym.*, 2011, **83**, 1652-1658. (e) K. Kolářová, V. Vosmanská, S. Rimpelová, V. Švorčík, *Cellulose,* 2013, 20(2), 953-961.

6 (a) Y. Sasai, Y. Yamauchi, S.-I. Kondo, M. Kuzuya, *Chem. Pharm. Bull.,* 2004, **52**(3), 339-344. (b) T. L. Ward, H. Z. Jung, O. Hinojosa, R. R. Benerito, *J. Appl. Polym. Sci.*, 1979, **23**, 1987-2003. (c) M. Kuzuya, K. Morisaki, J. Niwa, Y. Yamauchi, K. Xu, *J. Phys. Chem.*, 1994, **98**, 11301-11307.

7 Z. Q. Hua, R. Sitaru, F. Denes, R. A. Young, *Plasmas Polym.*, 1997, **2**(3), 199-224.

8 M. Benoit, A. Rodrigues, Q. Zhang, E. Fourré, K. De Oliveira Vigier, J.-M. Tatibouët, F. Jérôme, *Angew. Chem. Int. Ed.*, 2011, **50**(38), 8964-8967.

9 M. Benoit, A. Rodrigues, K. De Oliveira Vigier, E. Fourré, J. Barrault, J.-M. Tatibouët, F. Jérôme, *Green Chem.*, 2012, **14**(8), 2212 – 2215.

10 (a) R. Molina, P. Jovancic, S. Vilchez, T. Tzanov, C. Solans, *Carbohydr. Polym.*, 2014, **103**, 472-479. (b) A. Liguori, L. Paltrinieri, A. Stancampiano, C. Gualandi, M. Gherardi, V. Colombo, M. L. Focarete, *Plasma Process. Polym.*, 2015, DOI : 10.1002/ppap.201500054. (c) P. Deeyai, M. Suphantharika, R. Wongsagonsup, S. Dangtip, *Chin. Phys. Lett.*, 2013, **30**(1), 018103/1-018103/4

11 (a) Ganguli, S. *Worlds Poultry Sci. J.,* 2013, **69**, 639-647. (b) Ringø, E.; Olsen, R E. Olsen; Jensen, I.; Romero, J.; Lauzon H. L. *Rev. Fish Biol. Fisheries,* 2014, **24**, 1005-1032

12 40°c is the average temperature of the DBD reactor measured on the external surface of electrodes. It means that the temperature inside the DBD reactor might be slightly higher.

13 W. Zhang, H. He, X. Zhang, *Soil Biol. Biochem.*, 2007, **39**, 2665-2669.

14 E. Suárez-Pereira, E. M. Rubio, S. Pilard, C. Ortiz Mellet, J. M. García Fernández, *J. Agric. Food Chem.,* 2010, **58**, 1777–1787.

15 I. Ciucanu, C. E. Costello, *J. Am. Chem. Soc.*, 2003, **125**, 16213-16219.

16 J. S. Kim, B. L. Reuhs, F. Michon, R. E. Kaiser, R. G. Arumugham, *Carbohydr. Res.*, 2006, **341**, 1061-1064.

17 G. Sassaki, P. Gorin, L. Souza, P. Czelusniak, M. Lacomini, *Carbohydr. Res.,* 2005, **340**, 731-739.

18 (a) H. Kono, S. Yunoki, T. Shikano, M. Fujiwara, T. Erata, M. Takai, *J. Am. Chem. Soc.*, 2002, **124** (25), 7506–7511. (b) H. Kono, T. Erata, M. Takai, *J. Am. Chem. Soc.*, 2002, **124** (25), 7512-7518

19 A. Bagno , F. Rastrelli , G. Saielli *J. Org. Chem.*, 2007, **72**, 7373–7381.

20 Y. Sun, L. lin, H. Deng, J. Li, B. He, R. Sun, P. Ouyang, *Biores.*, 2008, **3**(2), 297-315.

21 W. Burchard, *Adv. Polym. Sci.*, 1999, **143**, 113-194.

22 (a) Y. Tao, L. Zhang, F. Yan, X. Wu, *Biomacromolecules,* 2007, 8, 2321-2328. (b) S. Wong, D. Appelhans, B. Volt, U. Scheler, *Macromolecules,* 2001, **34**, 678-680.

23 M. Kuzuya, Y. Yamauchi, *Thin Solid Films*, 1998, **316**, 158-164.

Green Chemistry

ARTICLE

Table of content

Fast and solvent free polymerization of carbohydrates induced by non-thermal atmospheric plasma

Joakim Delaux, Michaël Nigen, Elodie Fourré, Jean-Michel Tatibouët, Abdellatif Barakat, Loyda Atencio, José M. García Fernández, Karine De Oliveira Vigier and François Jérôme*
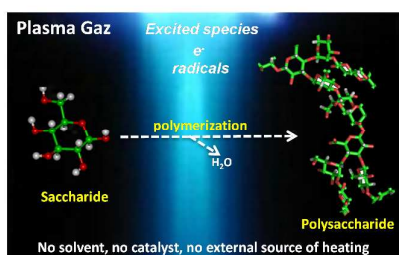
Non-thermal atmospheric plasma is capable of selectively polymerizing carbohydrates quasi instantaneously without assistance of any solvent or catalyst or external source